Post-therapy Marrow Changes

3

Jason H. Kurzer and Olga K. Weinberg

Bone marrow biopsies and aspirates from patients undergoing various forms of treatment can show a variety of histological and cytological findings, and it is therefore imperative that pathologists understand the array of associated therapy-related effects. Patients receiving induction chemotherapy for acute leukemia frequently have bone marrow aspirates and/or biopsies at specific intervals, allowing the pathologist to observe the immediate and long-term effects of the treatment regimen (Table 3.1).

Biopsies obtained after approximately 1 week of myeloablative therapy typically show marrow aplasia, loss of adipocytes, fibrinoid necrosis, and edema associated with dilated sinuses (Fig. 3.1) [1–3]. Two weeks after initiation of treatment, the fibrinoid necrosis persists, and the cellularity is composed of stromal cells, hemosiderin-laden macrophages, lymphocytes, and plasma cells (Figs. 3.2 and 3.3). At this time, adipocytes return, are frequently multiloculated, and are often accompanied by a loose network of reversible reticulin fibrosis (Fig. 3.4). By day 29 of induction therapy, erythropoiesis has typically returned, and may be accompanied by some degree of dyspoiesis (Fig. 3.5). Granulopoiesis typically follows, with megakaryopoiesis frequently appearing last (Figs. 3.6 and 3.7) [1].

It is important to recognize certain changes that may mimic residual disease after therapy. Hyperplasia of hematogones is often seen after treatment and can be particularly prominent in pediatric marrows following therapy and thus provide a diagnostic challenge when evaluating for residual lymphoblastic leukemia (Fig. 3.8). Other diagnostic challenges can arise when patients are treated with growth factors such as G-CSF. While early G-CSF therapy may show promyelocytic hyperplasia reminiscent of acute promyelocytic leukemia, these precursors typically show normal cytologic and histologic morphology (Figs. 3.9 and 3.10) [4–7]. Moreover, with time, the myeloid hyperplasia will demonstrate more mature precursors (Fig. 3.11). Another diagnostic challenge occurs in the setting of rituximab treatment. Therapy with rituximab can sometimes induce the formation of T-cell lymphoid aggregates in the marrow that may morphologically mimic persistent involvement by lymphoma (Fig. 3.12) [8].

Finally, certain diseases have specific therapies that show associated marrow findings. All *trans* retinoic acid (ATRA) treatment has been shown to promote differentiation of the atypical promyelocytes of acute promyelocytic leukemia (APL). Consequently, within a week of ATRA treatment, neutrophils may contain Auer rods. After several weeks, primary granules are diminished, but neutrophils may show deficiencies of secondary granule formation (Fig. 3.13) [9]. Chronic myeloid leukemia typically shows a hypercellular bone marrow with myeloid hyperplasia and frequent atypical megakaryocytes (Fig. 3.14). However, treatment for several months with a tyrosine kinase inhibitor such as imatinib can significantly reduce the marrow cellularity to normocellularity or even hypocellularity, as well as reduce the number of atypical megakaryocytes (Fig. 3.15) [10–12].

J.H. Kurzer (✉)
Stanford University School of Medicine, Stanford, CA, USA
e-mail: kurzer@stanford.edu

O.K. Weinberg
Pathology Department, Boston Children's Hospital,
Boston, MA, USA
e-mail: Olga.Weinberg@childrens.harvard.edu

T.I. George, D.A. Arber (eds.), *Atlas of Bone Marrow Pathology*, Atlas of Anatomic Pathology,
https://doi.org/10.1007/978-1-4939-7469-6_3

Table 3.1 Timeline of post-therapy changes in the bone marrow

Timepoint	Findings
One Week	Marrow aplasia
	Loss of adipocytes
	Fibrinoid necrosis
	Edema
	Dilated sinuses
Two Weeks	Fibrinoid necrosis
	Cellularity composed of stromal cells, hemosiderin-laden macrophages, lymphocytes, and plasma cells
	Return of adipocytes: multiloculated
	Loose network of reversible reticulin fibrosis
	Hematogone hyperplasia
Four Weeks	Erythroid precursors return
	Some granulopoiesis
	Clusters of megakaryocytes
	Reticulin fibrosis diminishes

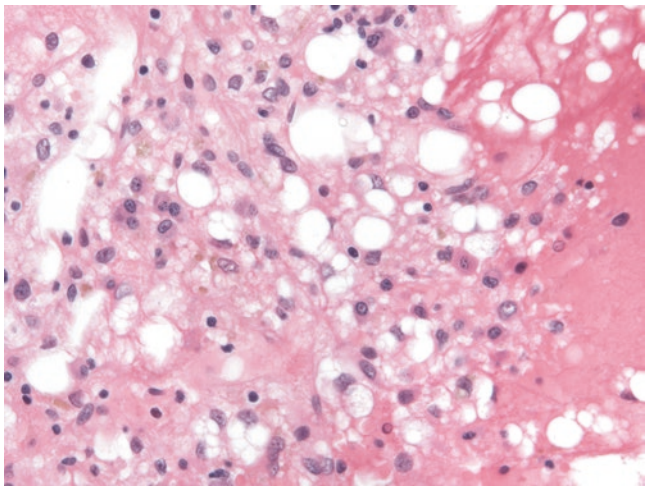

Fig. 3.2 This bone marrow biopsy of a 34-year-old man shows therapy-related changes on day 14, status post 7+3 induction therapy for acute myeloid leukemia. There continues to be prominent fibrinoid necrosis in the background. The cellularity is composed predominantly of lymphocytes, plasma cells, stromal cells, and histiocytes. A subset of histiocytes contains cellular debris and hemosiderin. By day 14, reemergence of adipocytes is appreciated, with many appearing multiloculated. A loose network of reticulin fibrosis can be appreciated in the background

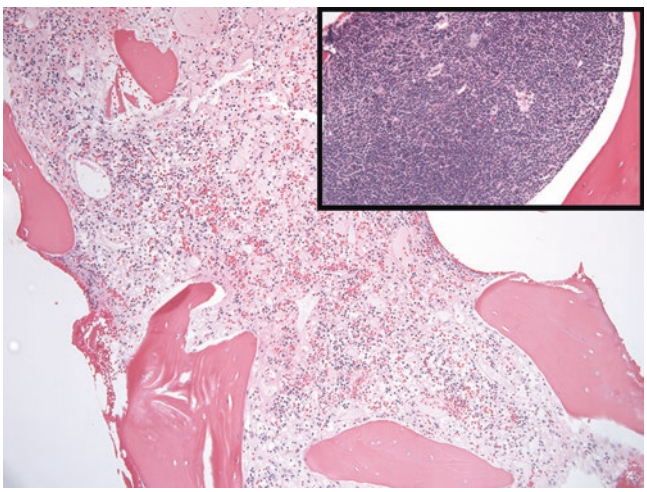

Fig. 3.1 This bone marrow biopsy of a 15-year-old female shows therapy-related changes on day 8 of induction chemotherapy for B-lymphoblastic leukemia. Prior to treatment, the marrow space is hypercellular and replaced by sheets of immature lymphoblasts (*inset*). On day 8 of induction therapy, the marrow is hypocellular and shows dilated sinuses with prominent edema, fibrinoid necrosis of stromal cells, an absence of hematopoietic precursors and adipocytes, and, in this case, multiple foci of residual scattered tumor cells

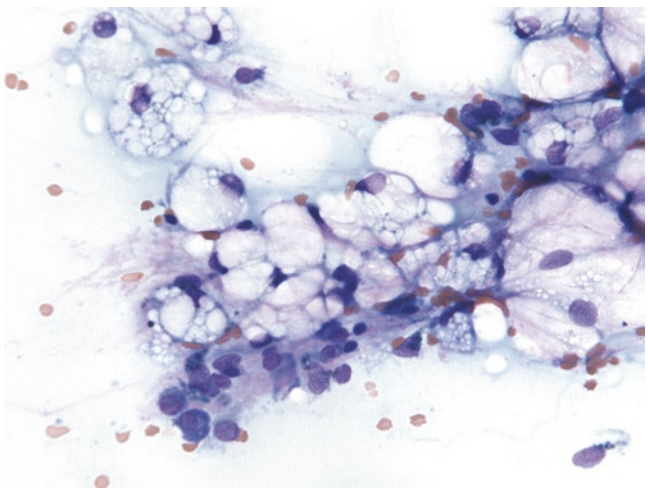

Fig. 3.3 This bone marrow aspirate from the patient in Fig. 3.2 shows multiloculated adipocytes, stromal cells, plasma cells, and occasional hemosiderin-laden macrophages

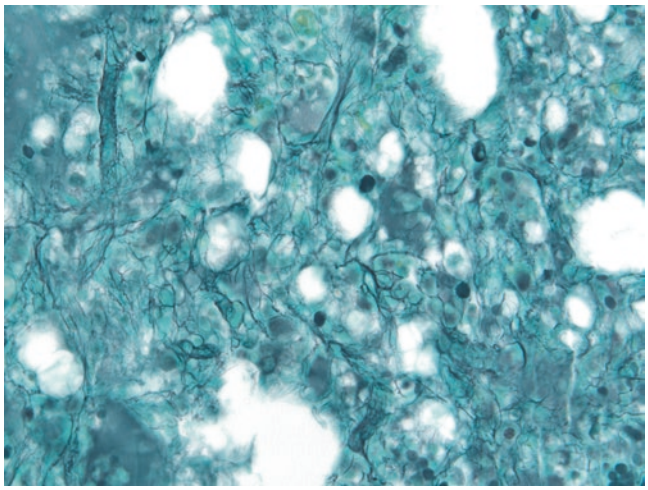

Fig. 3.4 This reticulin stain of the bone marrow biopsy of the patient from Fig. 3.2 shows increased fibrosis. Reversible reticulin fibrosis may sometimes be seen after high-dose chemotherapy

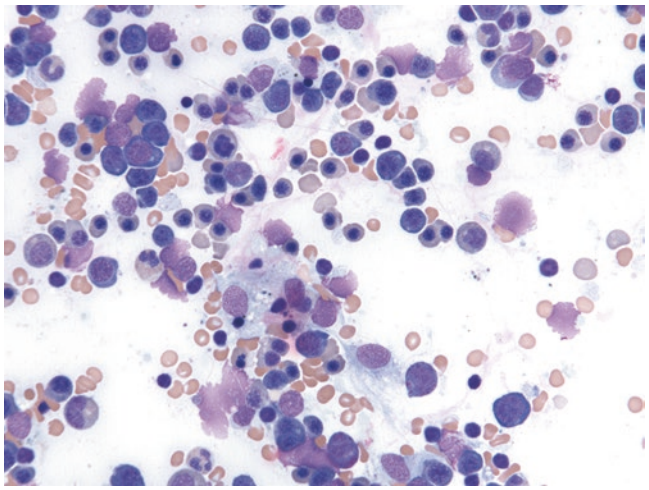

Fig. 3.6 This bone marrow aspirate of a 2-year-old boy shows therapy-related changes on day 29 of induction therapy for B-lymphoblastic leukemia. Erythroid-predominant hematopoiesis is appreciated, with occasional dyspoietic erythroblasts. Scattered immature granulocytes are also present in fewer numbers, indicative of returning myelopoiesis

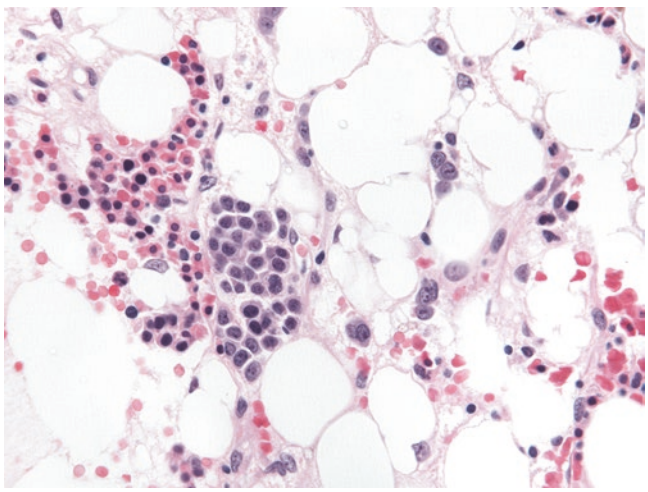

Fig. 3.5 This bone marrow biopsy of a 17-year-old male shows therapy-related changes on day 29 of induction therapy for B-lymphoblastic leukemia. As hematopoiesis returns, erythroid precursors are typically the first of the three lineages to reappear. It is not uncommon to find erythroid colonies scattered within a hypocellular marrow

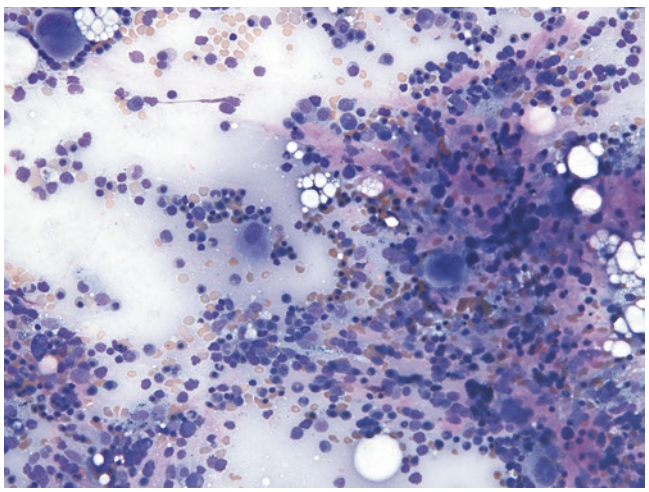

Fig. 3.7 This bone marrow aspirate of a 24-year-old man shows an erythroid hyperplasia on day 29 of induction therapy for B-lymphoblastic leukemia. Of note, regenerating megakaryocytes are present in clusters, with occasional hypolobated forms

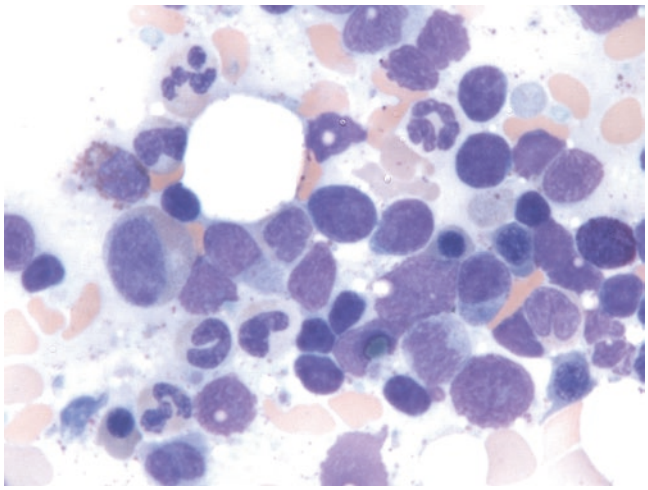

Fig. 3.8 This bone marrow aspirate of a 71-year-old man following treatment for acute myeloid leukemia shows a prominent hematogone hyperplasia admixed with maturing myeloid and erythroid precursors

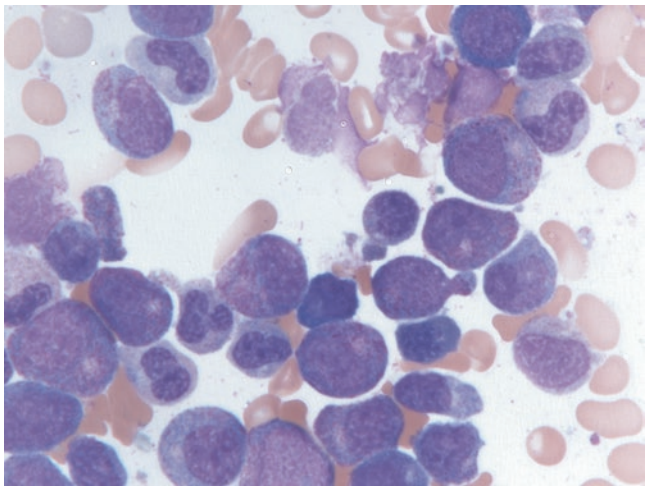

Fig. 3.10 The bone marrow aspirate from the same patient as Fig. 3.9 shows marked left-shifted maturation of the granulocytic precursors. A prominent Golgi apparatus is visible in the numerous normal-appearing promyelocytes, a finding that is commonly seen with G-CSF treatment

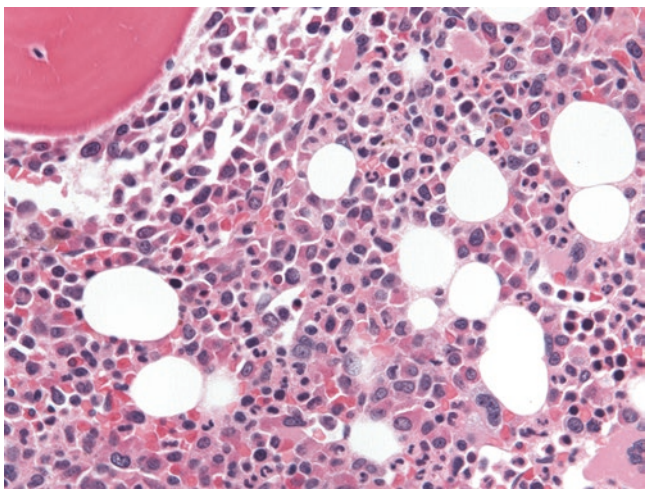

Fig. 3.9 This bone marrow from a 25-year-old woman treated with G-CSF 1 week prior to biopsy is hypercellular, with an increase in immature granulocytes. Nevertheless, a normal granulopoietic pattern is observed, proceeding outward from the bone trabeculae into the interstitium

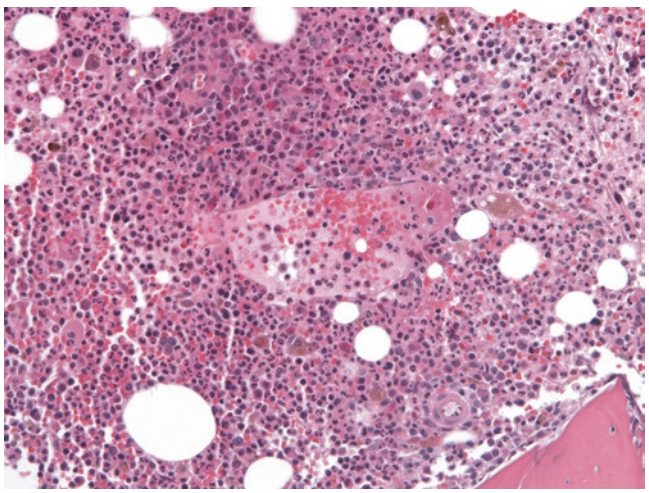

Fig. 3.11 This bone marrow from a 40-year-old man treated with G-CSF 2 weeks prior to biopsy shows a myeloid hyperplasia similar to Fig. 3.10 but with an increased percentage of fully mature granulocytes

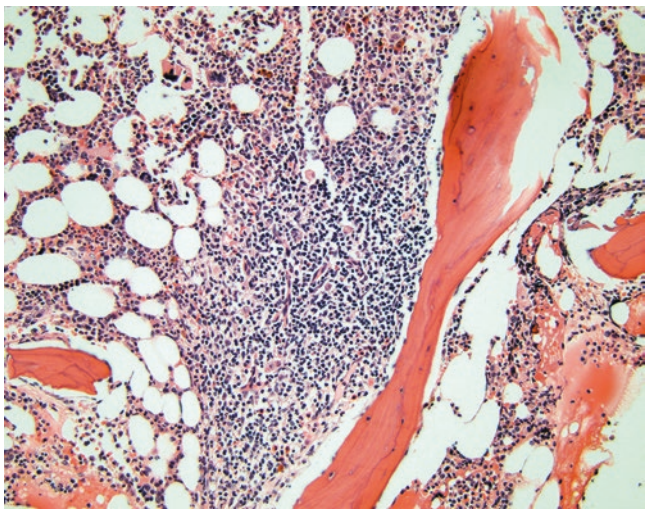

Fig. 3.12 This bone marrow biopsy from an 87-year-old woman with a history of diffuse large B-cell lymphoma shows prominent lymphoid aggregates in the marrow after receiving therapy that included rituximab. In this case, the lymphoid aggregates were shown to be composed of almost all T cells and virtually no B cells. As lymphoma cells with minimal CD20 expression may be present, it is important to stain for alternative B-cell markers such as PAX-5 or CD79a

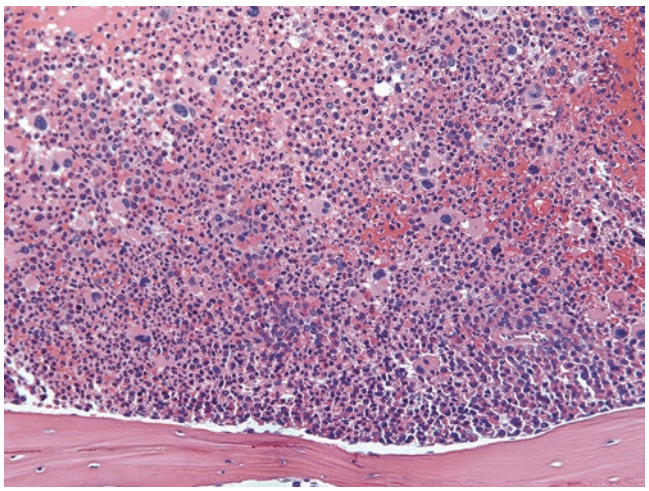

Fig. 3.14 This bone marrow biopsy from a 32-year-old woman with chronic myeloid leukemia shows the characteristic hypercellularity with associated myeloid hyperplasia. Loose clusters of atypical megakaryocytes are readily apparent

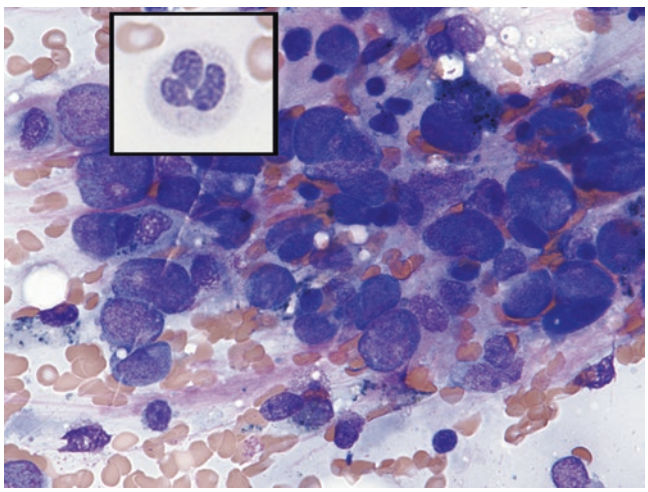

Fig. 3.13 This bone marrow aspirate from a 25-year-old woman treated with ATRA, idarubicin, and arsenic is hypocellular, with little differentiation of myeloid precursors past the promyelocytic stage, but the peripheral blood (inset) shows occasional neutrophils with a deficiency of secondary granules, likely resulting from ATRA-induced maturation of the initial neoplastic promyelocytes

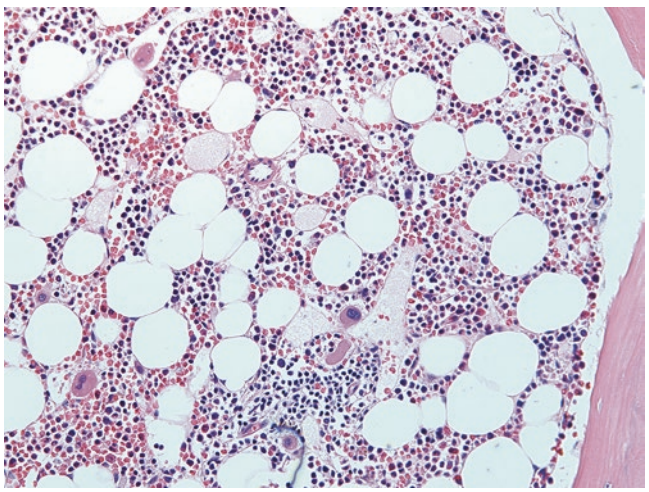

Fig. 3.15 This bone marrow biopsy from the same patient depicted in Fig. 3.14 reveals the effects of 6 months of imatinib treatment. The cellularity has returned to normal, with only scattered megakaryocytes

References

1. Islam A, Catovsky D, Galton DAG. Histological study of bone marrow regeneration following chemotherapy for acute myeloid leukemia and chronic granulocytic leukemia in blast transformation. Br J Haematol. 1980;45:535–40.
2. Dick FR, Burns CP, Weiner GJ, Heckman KD. Bone marrow morphology during induction phase of therapy for acute myeloid leukemia (AML). Hematol Pathol. 1995;9:95–106.
3. Kushwaha R, Kumar A, Aggrawal K, Nigam N, Kumar A. Post chemotherapy blood and bone marrow regenerative changes in childhood acute lymphoblastic leukemia: a prospective study. Indian J Pathol Microbiol. 2014;57:72–7. https://doi.org/10.4103/0377–4929.130903.
4. Campbell LJ, Maher DW, Tay DL, Boyd AW, Rockman S, McGrath K, et al. Marrow proliferation and the appearance of giant neutrophils in response to recombinant human granulocyte colony stimulating factor (rhG-CSF). Br J Haematol. 1992;80:298–304.
5. Ryder JW, Lazarus HM, Farhi DC. Bone marrow and blood findings after marrow transplantation and rhGM-CSF therapy. Am J Clin Pathol. 1992;97:631–7.
6. Schmitz LL, McClure JS, litz CE, Dayton V, Weisdorf DJ, Parkin JL, Brunning RD. Morphologic and quantitative changes in blood and marrow cells following growth factor therapy. Am J Clin Pathol. 1994;101:67–75.
7. Harris AC, Todd WM, Hackney MH, Ben-Ezra J. Bone marrow changes associated with recombinant granulocyte-macrophage and granulocyte colony-stimulating factors: discrimination of granulocytic regeneration. Arch Pathol Lab Med. 1994;118:624–9.
8. Raynaud P, Caulet-Maugendre S, Foussard C, Salles G, Moreau A, Rossi JF, et al. GOELAMS Group. T-cell lymphoid aggregates in bone marrow after rituximab therapy for B-cell follicular lymphoma: a marker of therapeutic efficacy? Hum Pathol. 2008;39:194–200.
9. Miyauchi J, Ohyashiki K, Inatomi Y, Toyama K. Neutrophil secondary-granule deficiency as a hallmark of all-trans retinoic acid-induced differentiation of acute promyelocytic leukemia cells. Blood. 1997;90:803–13.
10. Hasserjian RP, Boecklin F, Parker S, Chase A, Dhar S, Zaiac M, et al. ST1571 (imatinib mesylate) reduces bone marrow cellularity and normalizes morphologic features irrespective of cytogenetic response. Am J Clin Pathol. 2002;117:360–7.
11. Frater JL, Tallman MS, Variakojis D, Druker BJ, Resta D, Riley MB, et al. Chronic myeloid leukemia following therapy with imatinib mesylate (Gleevec). Bone marrow histopathology and correlation with genetic status. Am J Clin Pathol. 2003;119:833–41.
12. McNamara C, Grigg A, Szer J, Roberts A, Campbell L, Hoyt R, et al. Morphological effects of imatinib mesylate (STI571) on the bone marrow and blood of patients with Philadelphia chromosome (Ph) positive chronic myeloid leukaemia. Clin Lab Haematol. 2003;25:119–25.